GMR
The Original

MARINE MACROALGAL EXTRACT-FUNCTIONALIZED STARCH/PVA/CuO ELECTROSPUN NANOFIBROUS SCAFFOLDS WITH ENHANCED *IN VITRO* ANTI-INFLAMMATORY ACTIVITY

Rashmi TS[1], Rashmi Singh[2], Akanksha Singh[3], Krishnaswamy Ezhilan Vivekanandan[4], Preeti Suresh Kori[5], Chaithra R[6], Nagaveni VB[7]*

[1]Department of Biotechnology, Government Science College, Chitradurga - 577501, Karnataka, India. Email: rashuprabhu@gmail.com
[2]Department of Zoology, MMH College, Ghaziabad - 201009, Uttar Pradesh, India. Email: rashmirrsingh@gmail.com
[3]Department of Zoology, Dyal Singh College, University of Delhi, 110003, India. Email: singhakanksha.au@gmail.com
[4]Department of Microbiology, PSG College of Arts & science, Civil Aerodrome Post, Avinashi Road, Coimbatore- 641014, Tamil Nadu, India. Email: vivekanandanbiotech@gmail.com
[5]Government Science College, Chitradurga 577501, Karnataka. India. Email: preethikori06@gmail.com
[6]Department of Postgraduate Studies and Research in Biochemistry, Jnana Sahyadri, Kuvempu University, Shankaraghatta, Shivamogga- 577 451, Karnataka, India. Email: chaithra.rudrappa14@gmail.com
[7]Department of Chemistry, HPPC Government First Grade college Challakere - 577522, Karnataka. India. Email: manimohanvb@gmail.com
*Correspondence Author: Nagaveni VB, manimohanvb@gmail.com (N.V.B)

ABSTRACT
This study developed starch/PVA electrospun nanoscaffolds incorporating *Sargassum ilicifolium*-synthesized CuO NPs and assessed their anti-inflammatory potential. UV-Vis, Fourier Transform Infrared Spectroscopy (FTIR) and X-Ray Diffraction (XRD) confirmed nanoparticle formation and scaffold integration, while Scanning Electron Microscopy (SEM) revealed a porous fibrous morphology. Thermogravimetric Analysis (TGA) indicated thermal stability up to 374°C, and Dynamic Light Scattering (DLS) showed CuO NPs had a 137 nm average size with -18.3 mV zeta potential. In anti-inflammatory assays, nanoscaffolds exhibited dose-dependent inhibition, achieving 84.38% (protein denaturation) and 81.35% (xanthine oxidase) at 100 µg/mL-comparable to diclofenac sodium (85.78% and 82.78%). The nanoscaffolds outperformed standalone algal extract and CuO NPs, suggesting synergistic effects. These results underscore the scaffold's efficacy, attributed to enhanced bioavailability and controlled release, positioning it as a sustainable anti-inflammatory material. Further *in vivo* studies are warranted.

KEYWORDS: *Sargassum ilicifolium*, Green synthesis, CuO NPs, Starch/PVA/CuO-NPs nanoscaffolds, Anti-inflammatory activity.

1. INTRODUCTION

The rising global burden of chronic inflammatory diseases, including arthritis, cardiovascular disorders, and neurodegenerative conditions, has heightened the demand for safer, biocompatible, and eco-friendly therapeutic alternatives to conventional anti-inflammatory agents [1]. Despite the widespread use of synthetic drugs, such as non-steroidal anti-inflammatory drugs (NSAIDs), their prolonged administration often results in adverse side effects, including gastrointestinal toxicity, renal dysfunction, and cardiovascular complications [2]. Consequently, significant research efforts have been directed toward identifying naturally derived compounds and advanced delivery platforms that can offer effective anti-inflammatory benefits while minimizing undesirable outcomes [3]. In this context, the intersection of nanotechnology and marine-derived phytotherapeutics has emerged as a promising frontier in biomedical innovation, offering novel solutions for inflammation management [4].

Marine macroalgae, particularly brown algae belonging to the genus *Sargassum*, have garnered considerable attention due to their abundant and diverse repertoire of bioactive metabolites, including phenolics, terpenoids, flavonoids, and sulfated polysaccharides [5]. Among them, *Sargassum ilicifolium*, widely distributed in tropical intertidal zones, is a rich source of biologically active compounds exhibiting antioxidant, antimicrobial, anti-inflammatory, and anticancer properties [6]. Traditional medicinal practices in coastal communities have long utilized various species of *Sargassum* for treating inflammation-related ailments, which supports their potential as a source of therapeutic agents [7]. However, the conventional extraction of these bioactives often suffers from low efficiency and lengthy processing times [8]. The incorporation of ultrasonic-assisted extraction (UAE) presents a modern, efficient, and environmentally benign approach to enhance the yield and quality of these compounds by promoting cell wall disruption and improving solvent penetration [9].

Parallel to the advancement of marine-derived phytochemicals is the increasing utilization of green synthesis methodologies in nanotechnology [10]. Among various metal oxide nanoparticles, copper oxide nanoparticle (CuO NPs) has gained prominence due to its unique physicochemical properties and therapeutic relevance [11]. CuO NPs possess broad-spectrum antimicrobial and notable anti-inflammatory activities, making them ideal

candidates for integration into biomedical platforms [12]. Conventional physical and chemical synthesis routes of CuO, however, often involve toxic precursors and harsh conditions that compromise biocompatibility [13]. In contrast, the use of plant- or algal-mediated green synthesis offers a sustainable and eco-friendly alternative, where bioactive constituents serve as natural reducing and capping agents, leading to the formation of biocompatible nanostructures with enhanced therapeutic efficacy [2].

Recent studies have explored the potential of combining naturally synthesized metal oxide nanoparticles with polymer-based biomaterials to develop multifunctional nanocomposite scaffolds [14]. Among various biopolymers, starch—a naturally abundant, biodegradable polysaccharide—has emerged as a favorable candidate for scaffold fabrication owing to its excellent film-forming ability, biocompatibility, and capacity for chemical modification [15]. However, starch alone lacks sufficient mechanical strength and water stability, which can be effectively improved by blending it with synthetic polymers such as polyvinyl alcohol (PVA) [16]. PVA is a non-toxic, water-soluble synthetic polymer widely employed in biomedical applications for its mechanical integrity, flexibility, and ease of electrospinning [17]. The synergistic combination of starch and PVA thus creates an ideal matrix for fabricating nanofibrous scaffolds capable of sustained drug or nanoparticle delivery [18].

Electrospinning, a versatile and scalable technique for generating nanofibrous structures, mimics the architecture of natural extracellular matrices (ECM), thereby enhancing cell adhesion, proliferation, and tissue integration [19]. This method has gained traction in biomedical engineering for the fabrication of drug-loaded wound dressings, tissue engineering scaffolds, and anti-inflammatory platforms [20]. Incorporating biosynthesized CuO NPs into starch/PVA electrospun fibers can potentially augment the anti-inflammatory, antimicrobial, and antioxidant properties of the scaffold while maintaining its structural and mechanical stability [21]. Furthermore, the nanoscale architecture of electrospun fibers facilitates a large surface area-to-volume ratio, promoting effective interaction with biological environments and enhancing therapeutic efficacy [22].

The present study aims to fabricate and characterize novel starch/PVA-based electrospun nanofibrous scaffolds embedded with CuO NPs synthesized via an ultrasonic-assisted green route using *S. ilicifolium* extract. This research integrates three innovative elements: the application of ultrasonic-assisted extraction for the enhanced recovery of algal bioactives, the biogenic synthesis of CuO NPs, and their incorporation into a biodegradable nanofibrous scaffold via electrospinning [23]. The study also evaluates the physicochemical and morphological characteristics of both the synthesized CuO NPs and the nanofibrous scaffolds using advanced analytical techniques such as UV-Vis spectroscopy, Fourier Transform Infrared Spectroscopy (FTIR), X-Ray Diffraction (XRD), Scanning Electron Microscopy (SEM), Thermogravimetric Analysis (TGA), and zeta potential analysis [24].

To assess the biomedical potential of the fabricated nanoscaffolds, the study focuses on evaluating their *in vitro* anti-inflammatory efficacy using protein denaturation inhibition and xanthine oxidase inhibition assays [25]. These models provide a reliable indication of the scaffold's capacity to suppress inflammatory pathways by targeting protein unfolding and reactive oxygen species generation, respectively [26]. The comparative analysis of anti-inflammatory activities between the algal extract, free CuO NPs, and CuO-loaded scaffolds offers insights into the added therapeutic value of integrating green-synthesized nanomaterials into polymeric matrices.

2. MATERIALS AND METHODS

2.1. Collection and preparation of marine macroalgae

Specimens of the brown macroalga *S. ilicifolium* were manually collected from the intertidal regions near Rameswaram, India. To preserve their bioactive constituents, the freshly gathered algae were promptly placed in ice-chilled containers for transportation to the laboratory. Upon arrival, the samples underwent thorough rinsing with tap water to eliminate sand, debris, and epiphytic organisms, followed by multiple washes with distilled water to ensure complete purification. The cleansed algal material was then chopped into small fragments and air-dried in the shade at ambient room temperature for approximately 14 days. Once fully dried, the seaweed was ground into a fine powder using a mechanical grinder and stored in airtight containers at room temperature for subsequent extraction processes.

2.2. Ultrasonic-Assisted Extraction of bioactive compounds

To extract bioactive compounds, 2 grams of the powdered *S. ilicifolium* were mixed with 50 mL of Milli-Q water. The mixture was subjected to ultrasonic treatment using a LABQUEST ultrasonic cleaner (Borosil; Serial No. 941032329018) at 60°C for 45 minutes. This process facilitated cell wall disruption and enhanced the release of intracellular substances. Post-sonication, the extract was filtered through sterile Whatman No. 1 filter paper to remove particulate matter, yielding a clear solution. The filtrate was stored at 10°C for immediate use and subsequently freeze-dried to obtain a dry extract powder suitable for nanoparticle synthesis [27].

2.3. Green synthesis of CuO NPs

CuO NPs were synthesized using a green approach, leveraging the reducing agents present in the *S. ilicifolium* extract. A solution of 50 mL of 0.1 M copper sulfate pentahydrate ($CuSO_4 \cdot 5H_2O$) was combined with 10 mL of the algal extract, prepared by dissolving 10 mg of lyophilized powder in Milli-Q water. The mixture, maintaining a 5:1 volume ratio, was stirred continuously at 650 rpm and maintained at 60°C for 2 hours. A visible color change from blue to bluish-green indicated the formation of CuO NPs. The resulting suspension was centrifuged and washed three times with double-distilled water to remove residual biomolecules and unreacted salts. The purified nanoparticles were freeze-dried for 48 hours and stored in a desiccator for further use in scaffold fabrication [28].

2.4. Fabrication of CuO-embedded starch/PVA nanofibrous mats via electrospinning

To create composite nanofibrous scaffolds, a 15% (w/w) aqueous solution of PVA was prepared by dissolving PVA in Milli-Q water under constant stirring until complete dissolution. Subsequently, 100 mg each of starch and the biosynthesized CuO NPs were dispersed into this PVA solution. The mixture was stirred vigorously at 50°C for 2.5 hours to achieve a homogeneous distribution and ensure proper integration of nanoparticles with the polymer matrix. The final uniform solution was loaded into a syringe fitted with a stainless-steel needle (0.84 mm internal diameter) and mounted on a HOLMARC HO-NFES-040 electrospinning machine. Electrospinning parameters were optimized as follows: voltage of 11.5 kV, a needle-to-collector distance of 12.3 cm, and a flow rate of 0.4 mL/h. The process was carried out at room temperature for 6–8 hours to produce nanofibrous mats, which were then peeled from the collector and stored under desiccated conditions for further analysis [29-31].

2.5. Physicochemical characterization of nanoparticles and nanofibrous scaffolds

2.5.1. UV-visible spectroscopy

The optical properties and surface plasmon resonance (SPR) of the CuO NPs and *S. ilicifolium* extract were assessed using a VIS SPEC V-730 UV-Visible spectrophotometer. Spectra were recorded between 200 and 800 nm, with deionized water serving as the blank. Characteristic absorption peaks indicative of nanoparticle formation were analyzed [32].

2.5.2. FTIR analysis

Functional group identification was performed using FTIR spectroscopy in Attenuated Total Reflectance (ATR) mode with a PerkinElmer Spectrum Two instrument. Spectra for CuO nanoparticles and the composite scaffolds were recorded over the range of 4000–400 cm^{-1} at a resolution of 4 cm^{-1}, averaging 64 scans per sample. The data provided insights into the interactions of functional groups such as phenolics, hydroxyls, carbonyls, and metal-oxygen bonds [33].

2.5.3. XRD analysis

The crystallographic structure and phase purity of CuO NPs and scaffold composites were determined using a Bruker D8 Advance XRD system with CuKα radiation (λ = 1.5406 Å), operating at 40 kV and 40 mA. Diffraction patterns were recorded over 2θ angles from 5° to 90° with a step size of 0.029649°. Phase analysis was performed by comparing peaks with standard JCPDS reference files [34].

2.5.4. SEM analysis

Morphological characterization of nanoparticles and nanofibrous scaffolds was conducted using a JEOL JSM-IT800 NANO scanning electron microscope. Prior to imaging, samples were coated with a thin gold layer via sputtering to enhance conductivity. SEM images were analyzed to assess fiber morphology, nanoparticle distribution, and surface topology [35].

2.5.5. TGA analysis

Thermal stability and decomposition profiles of the scaffolds were evaluated using a PerkinElmer TGA 8000 instrument. Approximately 5 mg of each sample was heated from ambient temperature to 550°C at a ramp rate of 15°C/min under a nitrogen atmosphere. Thermograms provided information on moisture loss, polymer degradation, and residual inorganic content [36].

2.5.6. Zeta potential and particle size

The colloidal stability and size distribution of CuO NPs were measured using a Malvern Zetasizer Ultra. Zeta potential values indicated electrostatic repulsion and nanoparticle stability in suspension, with higher absolute values corresponding to better dispersion [37].

All raw data and characterization results are accessible via the Mendeley Data repository at DOI: 10.17632/4kdtskdtmc.3.

2.6. Anti-inflammatory assays

2.6.1. Protein denaturation inhibition assay

The anti-inflammatory efficacy of the samples was assessed using a modified heat-induced protein denaturation assay. Each test mixture consisted of 0.45 mL of 5% aqueous bovine serum albumin and 0.05 mL of the test sample (algal extract, CuO NPs, starch/PVA/CuO scaffolds, or diclofenac sodium) at concentrations of 25, 50, 75, and 100 µg/mL. The pH was adjusted to 6.3 with 1 N HCl, followed by incubation at 37°C for 20 minutes. Subsequently, the tubes were heated at 57°C for 3 minutes and cooled to room temperature. Turbidity due to protein denaturation was measured spectrophotometrically at 660 nm [38].

2.6.2. Xanthine oxidase inhibition assay

Xanthine oxidase inhibitory activity was evaluated following a slightly modified standard protocol. The reaction mixture included 0.3 mL of each sample (algal extract, CuO NPs, starch/PVA/CuO scaffolds, or diclofenac sodium) at varying concentrations (25, 50, 75, and 100 µg/mL), 0.5 mL of 0.15 mM xanthine solution (prepared in phosphate buffer, pH 7.5), and 0.2 mL of xanthine oxidase enzyme (0.1 units/mL). After 15 minutes of incubation at 25°C, the absorbance was recorded at 295 nm. A blank lacking the enzyme was used as a control [39].

2.7. Statistical analysis

Experimental data were evaluated using SPSS v25.0 and GraphPad Prism v9.0. All assays were performed in triplicate, and results were expressed as mean ± standard deviation. One-way ANOVA followed by Tukey's or Dunnett's post-hoc tests was used to assess statistical significance ($p < 0.05$). Data normality was examined using the Shapiro–Wilk test [40].

3. RESULTS

3.1. UV–visible spectroscopy

The UV–Visible spectral characterization (Fig. 1) of the *S. ilicifolium* extract and synthesized CuO NPs (NPs) was performed using a JASCO V-730 UV-Vis spectrophotometer within a wavelength span of 200–800 nm and a 1 nm increment rate. The *S. ilicifolium* extract exhibited specific absorption peaks, indicative of its unique phytochemical constituents. In contrast, the CuO NPs presented prominent SPR bands, validating the formation of metal oxide nanoparticles. The instrument utilized continuous scan mode, maintained a 1.0 nm bandwidth, and incorporated baseline correction to ensure measurement precision. Both test samples were analyzed under consistent experimental settings using deionized water as the blank. These spectral profiles confirm successful CuO NPsynthesis and delineate the phytochemical characteristics of the *S. ilicifolium* extract.

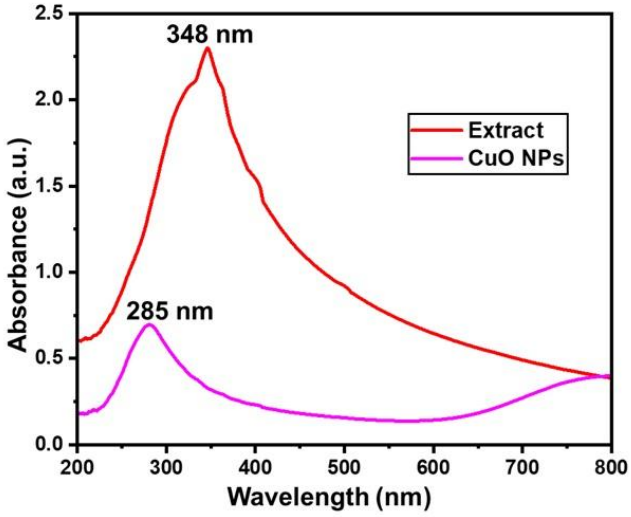

Fig. 1. UV–Visible spectral profiles of algal extract and CuO NPs.

3.2. FTIR analysis

FTIR spectroscopy (Fig. 2) of CuO NPs and starch/PVA electrospun nanoscaffolds was recorded using a PerkinElmer Spectrum IR system in Attenuated Total Reflectance (ATR) mode. The CuO NPs exhibited characteristic absorption bands at 2001.38, 1651.25, 1205.19, 866.65, 599.74, and 3128.62 cm^{-1}, which correspond to Cu–O bonds and surface functional moieties. Meanwhile, starch/PVA scaffolds showed distinct spectral bands at 3297.43 cm^{-1} (O–H stretch), 1710.65 cm^{-1} (C=O carbonyl stretch), 919.77 cm^{-1} (C–O–C polysaccharide stretching), and 842.91 cm^{-1} (C–H bending), confirming the presence of polymeric and carbohydrate constituents. Spectra were recorded across 4000 to 400 cm^{-1} with a resolution of 4 cm^{-1} over 64 scans. Notable shifts and broadening of peaks suggest interactions between phenolic, hydroxyl, and carbonyl groups, indicating the effective integration of CuO NPs within the scaffold matrix.

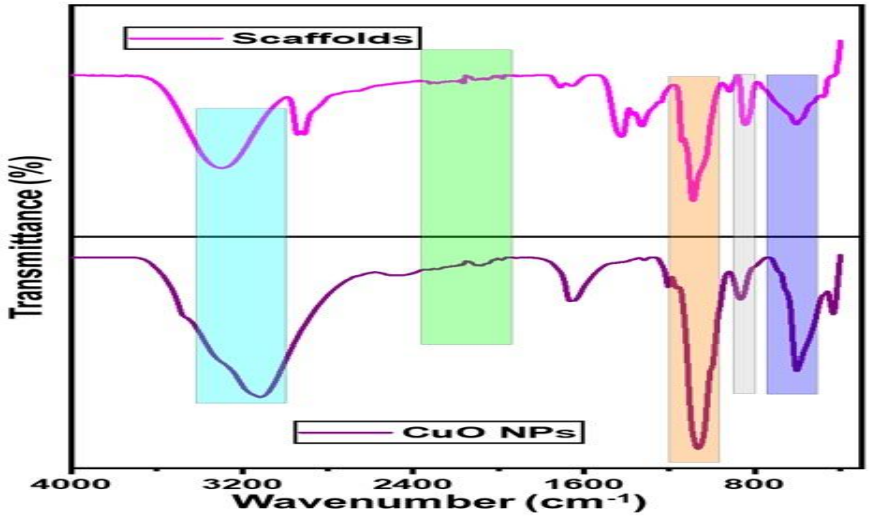

Fig. 2. FTIR spectra of CuO NPs and their incorporation into nanoscaffolds.

3.3. XRD analysis

XRD patterns (Fig. 3) of CuO NPs and starch/PVA nanoscaffolds were analyzed using a Bruker D8 Advance diffractometer equipped with CuKα radiation (λ = 1.5406 Å) at 40 kV and 40 mA. CuO NPs showed distinct reflections at 2θ angles of 16.258°, 22.278°, 26.286°, 28.070°, 29.112°, 32.792°, 37.236°, 44.982°, 48.168°, 51.879°, and 53.557°, consistent with the monoclinic phase of CuO as per JCPDS 80-1917. Crystallite sizes were

computed using the Scherrer equation. Starch/PVA nanoscaffolds showed broad peaks at 21.676°, 29.202°, 30.751°, 35.842°, 39.237°, 43.073°, 47.427°, 48.386°, and 57.535°, reflecting a semi-crystalline structure with d-spacing ranging from 4.09671 Å to 1.60059 Å. The CuO NPs displayed sharp and narrow peaks (FWHM 0.198°–0.861°), indicative of high crystallinity, whereas broader peaks in the nanoscaffolds (FWHM 0.100°–0.658°) reflect lower crystallinity. These results affirm phase purity and successful incorporation of CuO into the scaffold within a scan range of 5°–90° and step size of 0.029649°.

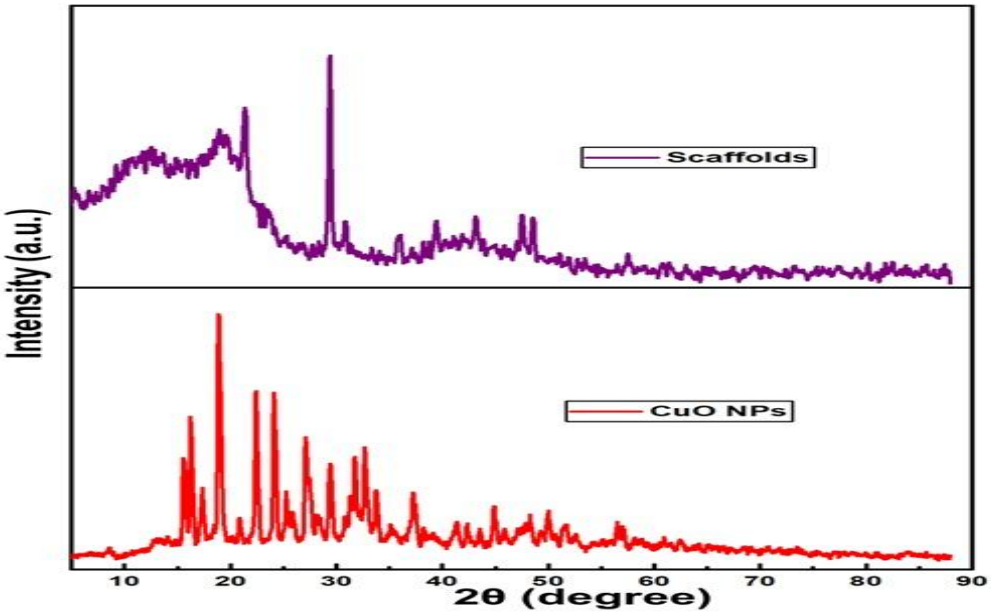

Fig. 3. XRD patterns of synthesized CuO NPs and CuO-loaded scaffolds.

3.4. SEM analysis

Surface morphology was evaluated via scanning electron microscopy (Fig. 4) using a JEOL JSM-IT800 NANO system. Prior to imaging, samples were gold-coated to improve conductivity. SEM images of CuO NPs revealed aggregated formations ranging from spherical to irregular geometries with rough surface features, implying crystalline structure. The starch/PVA electrospun scaffolds exhibited a well-organized, porous fibrous structure with consistent fiber diameters, demonstrating efficient electrospinning. The fibers appeared smooth and showed minimal bead formation, highlighting effective polymer blending and optimal electrospinning parameters. These high-resolution micrographs offer critical morphological data, supporting the materials' potential for biomedical and catalytic utilization.

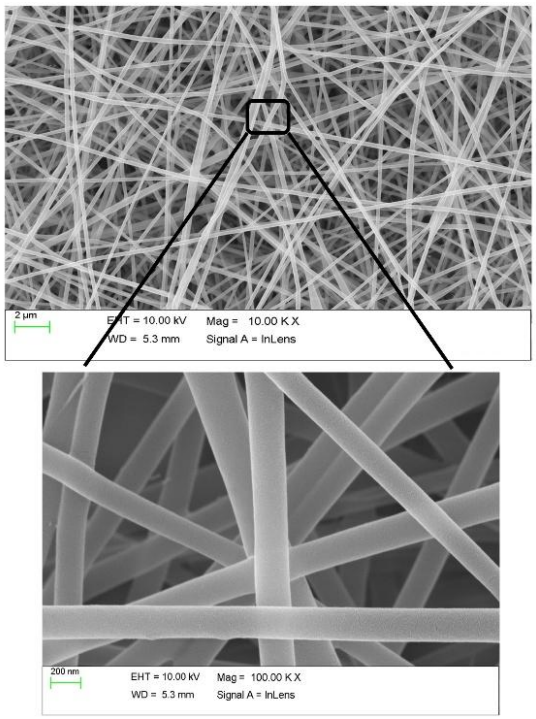

Fig. 4. SEM analysis of synthesized CuO NPs and CuO-loaded scaffolds.

3.5. TGA

Thermal stability of starch/PVA electrospun scaffolds was assessed by TGA using a PerkinElmer TGA 8000 analyzer (Fig. 5). A 3.110 mg sample was subjected to thermal scanning from 30°C to 550°C at a rate of 15°C/min. Initial thermal degradation began at 232.27°C, with the peak degradation rate observed at 327.56°C and final decomposition completed near 374.23°C. The total mass loss was calculated as 38.301%. The TGA curve indicated a preliminary weight reduction due to moisture evaporation and polymer chain decomposition, followed by substantial degradation at higher temperatures. These findings confirm the thermal resilience and degradation characteristics essential for scaffold-based applications.

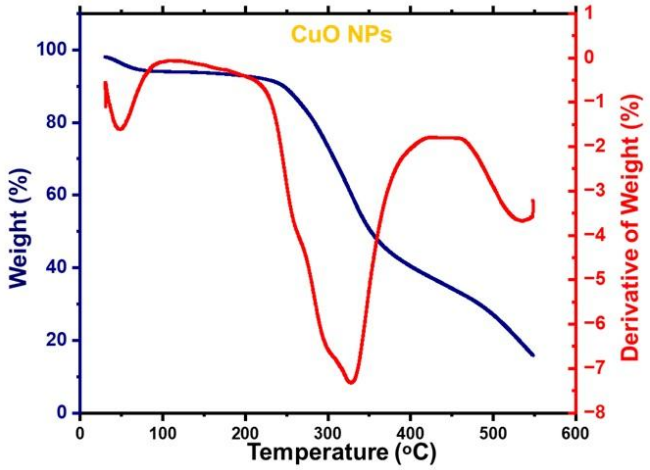

Fig. 5. Thermal degradation behavior of CuO-incorporated nanoscaffolds.

3.6. Zeta potential and particle size analysis

Particle size and colloidal behavior of CuO NPs were evaluated using Dynamic Light Scattering (DLS) with a Malvern Zetasizer Ultra. The measured average hydrodynamic diameter (Z-average) was 137 nm (Fig. 6), while the polydispersity index (PDI) stood at 0.7317, suggesting a moderately heterogeneous size profile. Zeta potential analysis at 25°C revealed a mean value of −18.3 mV, with secondary peaks at −29.14 mV and −14.58 mV (Fig. 7), indicating moderate electrostatic repulsion and dispersion stability. The conductivity of the suspension was recorded at 0.05074 mS/cm, and the quality factor of 5.22 supported the reliability of measurements. These observations demonstrate the CuO NPs' moderate colloidal stability and size diversity, reinforcing their suitability for applications in catalysis, biosensing, and medicine.

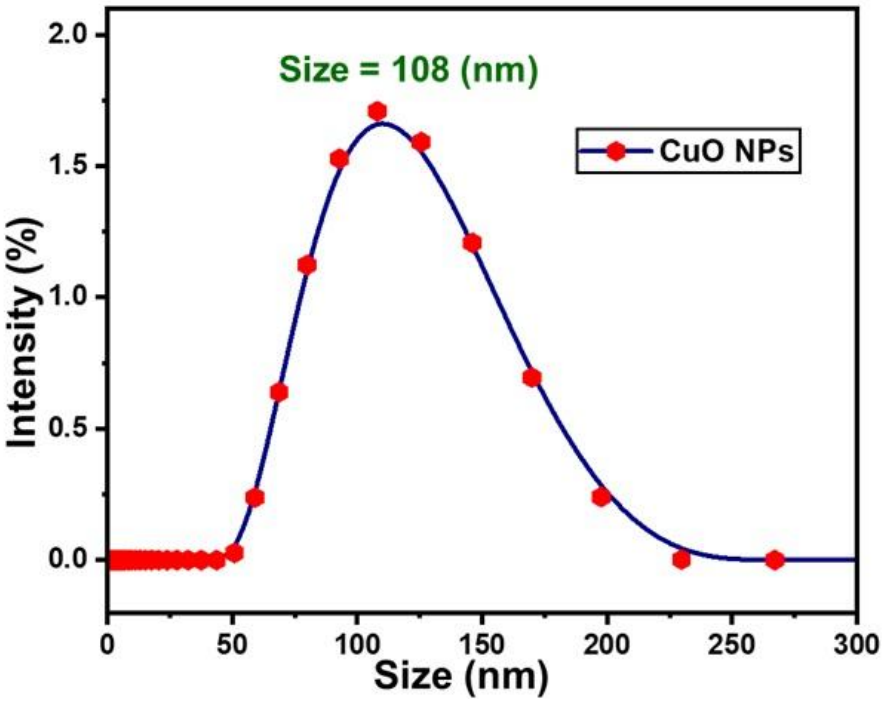

Fig.6. DLS particles size analysis of CuO NPs

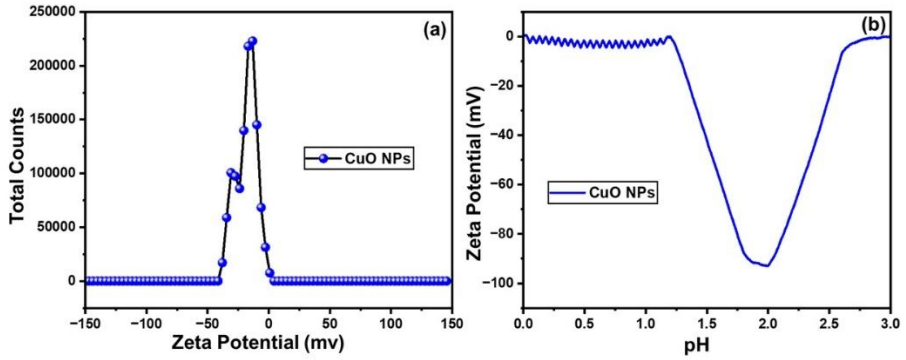

Fig.7. Zeta-potential analysis of CuO NPs

3.7. Anti-inflammatory assays

3.7.1. Protein denaturation inhibition assay

The anti-inflammatory potential of algal extract, CuO NPs, and starch/PVA/CuO-NPs nanoscaffolds was evaluated using the protein denaturation inhibition assay (Fig. 8). At a concentration of 25 µg/mL, the algal extract exhibited 24.17% inhibition, while CuO NPs and nanoscaffolds showed 28.17% and 31.17% inhibition, respectively. The standard drug (diclofenac sodium) recorded 28.84% inhibition at the same concentration. As the concentration increased to 50 µg/mL, the inhibition percentages rose to 39.58% for the extract, 43.58% for CuO NPs, and 45.58% for nanoscaffolds, compared to 43.80% for the standard. At 75 µg/mL, the nanoscaffolds demonstrated superior activity (67.70%) over CuO NPs (63.70%) and the extract (58.70%), while the standard achieved 65.30%. At the highest concentration (100 µg/mL), the nanoscaffolds exhibited remarkable inhibition (84.38%), surpassing both the extract (68.38%) and CuO NPs (74.38%), with the standard at 85.78%.

In a replicate experiment, similar trends were observed. The extract showed 22.15% inhibition at 25 µg/mL, while CuO NPs and nanoscaffolds recorded 28.15% and 30.15%, respectively, compared to the standard (30.33%). At 100 µg/mL, the nanoscaffolds (81.35%) outperformed the extract (67.35%) and CuO NPs (74.35%), though the standard remained the most effective (82.78%). These results highlight the dose-dependent anti-inflammatory activity of all test samples, with nanoscaffolds consistently exhibiting higher efficacy than the extract and CuO NPs, approaching the standard drug's performance.

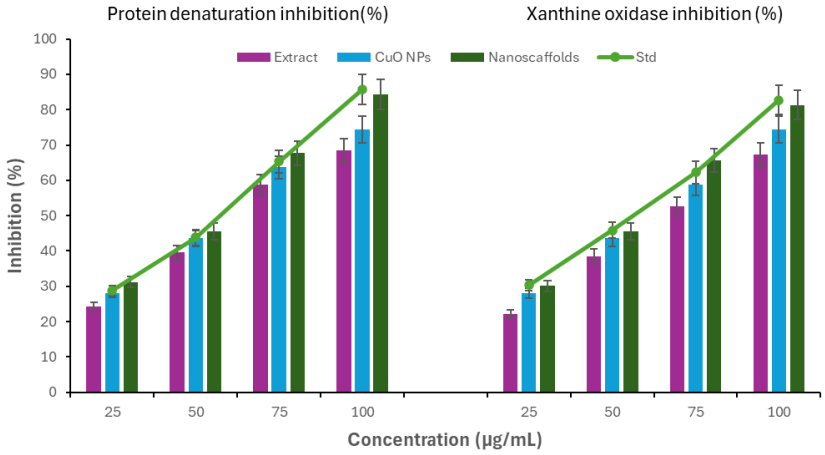

Fig.8. Anti-inflammatory activity analysis of algal extract, CuNPs and starch/PVA/CuONPs nanoscaffolds

3.7.2. Xanthine oxidase inhibition assay

The xanthine oxidase inhibition assay (Fig. 8) further validated the anti-inflammatory properties of the test samples. At 25 µg/mL, the algal extract, CuO NPs, and nanoscaffolds displayed inhibition percentages of 24.17%, 28.17%, and 31.17%, respectively, compared to the standard's 28.84%. Increasing the concentration to 50 µg/mL enhanced the inhibition to 39.58% (extract), 43.58% (CuO NPs), and 45.58% (nanoscaffolds), while the standard reached 43.80%. At 75 µg/mL, the nanoscaffolds (67.70%) again showed higher activity than CuO NPs (63.70%) and the extract (58.70%), with the standard at 65.30%. The trend continued at 100 µg/mL, where nanoscaffolds (84.38%) nearly matched the standard (85.78%), outperforming CuO NPs (74.38%) and the extract (68.38%).

In the replicate assay, the extract's inhibition at 25 µg/mL was 22.15%, while CuO NPs and nanoscaffolds achieved 28.15% and 30.15%, respectively, compared to the standard (30.33%). At 100 µg/mL, the nanoscaffolds (81.35%) demonstrated superior inhibition to the extract (67.35%) and CuO NPs (74.35%), though the standard remained the most potent (82.78%). These findings underscore the nanoscaffolds' enhanced anti-inflammatory activity, likely due to the synergistic effects of starch/PVA and CuO NPs, which improve bioavailability and interaction with inflammatory markers.

Both assays confirmed the dose-dependent anti-inflammatory effects of the algal extract, CuO NPs, and starch/PVA/CuO-NPs nanoscaffolds. The nanoscaffolds exhibited the highest inhibitory activity, often comparable to the standard drug, suggesting their potential as effective anti-inflammatory agents. The results align with the hypothesis that composite nanoscaffolds enhance therapeutic efficacy, possibly due to improved stability and controlled release of active components. Further studies are warranted to explore their mechanisms and *in vivo* applicability.

4. DISCUSSION

The comprehensive characterization and biological evaluation of *S. ilicifolium*-mediated CuO NPs and their integration into starch/PVA-based electrospun nanoscaffolds present compelling evidence for their potential in biomedical applications, particularly in anti-inflammatory therapies. The successful synthesis and incorporation of CuO NPs were validated through a series of instrumental analyses, each contributing crucial insights into the physicochemical and functional attributes of the developed nanomaterials.

The UV–Visible spectroscopic analysis provided an initial indication of the formation of CuO NPs. The *S. ilicifolium* extract demonstrated distinct absorption bands, attributed to various phytoconstituents such as flavonoids and phenolics. In contrast, the synthesized CuO NPs displayed characteristic SPR peaks in the UV-visible range, which is a hallmark feature of metal oxide nanoparticles. This confirms not only the successful reduction of copper ions by the algal extract but also the presence of bioactive compounds acting as reducing and capping agents. The precise and reproducible acquisition of spectra, enabled by instrument settings like continuous scan mode and 1.0 nm bandwidth, further ensured the reliability of the findings [41-47].

FTIR spectroscopy provided molecular-level insights into the interaction between CuO NPs and the polymeric matrix. The CuO NPs exhibited peaks corresponding to Cu–O vibrations and other surface functional groups. Simultaneously, the starch/PVA nanoscaffolds revealed characteristic bands indicative of hydroxyl, carbonyl, and polysaccharide moieties. Notably, the shifts in absorption peaks upon incorporation of CuO NPs into the scaffold imply successful chemical integration. These interactions may result from hydrogen bonding or electrostatic attraction between the functional groups of the polymer and the CuO surfaces, potentially enhancing the stability and performance of the composite scaffolds [48-53].

XRD analysis corroborated the crystalline nature of CuO NPs, displaying sharp diffraction peaks consistent with the monoclinic CuO phase as per the JCPDS 80-1917 reference. The calculated crystallite sizes confirmed nanometric dimensions, essential for biomedical functionality. The starch/PVA nanoscaffolds exhibited broader peaks, signifying their semi-crystalline nature, which is advantageous for flexibility and degradation kinetics. The maintained diffraction signatures of CuO in the composite indicate the nanoparticles retained their crystallinity post-incorporation. This is critical for applications where crystallinity influences catalytic or bioactive performance [54-61].

SEM served as an invaluable tool to visualize the morphological features of both CuO NPs and the electrospun scaffolds. The nanoparticles appeared aggregated with a mix of spherical and irregular shapes, likely resulting from phytochemical-mediated synthesis without surfactants. Meanwhile, the nanoscaffolds displayed uniform, bead-free fibers with well-defined porosity, a direct consequence of optimized electrospinning parameters. Such morphology enhances cell attachment and nutrient diffusion, making them ideal candidates for wound healing or tissue engineering. The integration of CuO NPs did not compromise fiber integrity, which reinforces the compatibility between inorganic and organic phases [62-69].

TGA provided crucial insights into the thermal stability of the composite scaffolds. The initial weight loss, corresponding to moisture evaporation, was followed by major decomposition phases related to the degradation of starch and PVA. The final decomposition near 374°C suggests that the scaffolds can withstand moderate thermal stress, a desirable property for biomedical packaging or drug delivery systems. The observed stability reflects successful cross-linking and interaction between polymer chains and CuO NPs, contributing to a thermally resilient composite matrix [70-74].

DLS and zeta potential analysis offered a quantitative assessment of the particle size distribution and colloidal stability of the synthesized CuO NPs. The average hydrodynamic size of 137 nm, coupled with a polydispersity index (PDI) of 0.7317, indicates moderate heterogeneity, which is typical for biogenic nanoparticles. The zeta potential value of −18.3 mV suggests that the nanoparticles possess sufficient surface charge to resist aggregation, albeit moderately. These findings point to a reasonably stable colloidal suspension, suitable for integration into polymer matrices and relevant for biological applications where dispersion stability influences cellular interactions [75-78].

Biological evaluation via anti-inflammatory assays reinforced the therapeutic potential of the developed materials. In the protein denaturation and xanthine oxidase inhibition assays, the starch/PVA/CuO-NPs nanoscaffolds consistently outperformed both the *S. ilicifolium* extract and standalone CuO NPs. The inhibition percentages exhibited a clear dose-dependent trend, with nanoscaffolds nearly matching the efficacy of the standard drug, diclofenac sodium, at higher concentrations. These results underscore the synergistic action of CuO NPs with the polymer matrix, possibly resulting from improved bioavailability and prolonged interaction with inflammatory mediators. The nanoscaffolds' enhanced surface area and sustained release capacity may have also contributed to their superior performance [79-81].

Overall, the multidisciplinary analysis spanning spectroscopy, microscopy, crystallography, and biological assays confirms the successful development of a composite nanoscaffold with promising anti-inflammatory capabilities. The phytochemical-mediated synthesis of CuO NPs ensures eco-friendliness, while their effective integration into biopolymeric scaffolds enhances functionality and application scope. The observed thermal, structural, and morphological features align with the requirements for advanced biomedical devices, particularly in wound care, drug delivery, and anti-inflammatory therapies. Future studies should explore *in vivo* models to validate these findings and uncover mechanistic insights into the therapeutic effects.

5. CONCLUSION

This study successfully demonstrated the fabrication of starch/PVA electrospun nanoscaffolds embedded with biogenically synthesized CuO NPs using *S. ilicifolium* extract. Comprehensive characterization techniques, including UV–Vis, FTIR, XRD, SEM, and TGA, confirmed the formation, integration, and stability of the CuO NPs within the nanoscaffold matrix. The nanoscaffolds exhibited a porous fibrous morphology, moderate crystallinity, and favorable thermal resistance, making them suitable for biomedical applications. Zeta potential and DLS analysis revealed moderately stable CuO NPs with a heterogeneous size distribution. *In vitro* anti-inflammatory assays (protein denaturation and xanthine oxidase inhibition) demonstrated a clear dose-dependent inhibition, with the starch/PVA/CuO nanoscaffolds consistently outperforming the algal extract and CuO NPs alone. Their activity closely approached that of the standard drug, suggesting a synergistic therapeutic effect. Overall, these findings highlight the nanoscaffolds' potential as promising anti-inflammatory biomaterials. Future *in vivo* evaluations and mechanistic studies will further validate their application in biomedical and pharmaceutical domains.

Data Availability Statement: The full dataset of physiochemical characterization associated with this work is published in Mendeley Data **[Dataset]** Innovative green composites: Material characterization of starch-based nanoscaffolds reinforced with *Sargassum ilicifolium*-mediated copper oxide nanostructures (DOI: 10.17632/4kdtskdtmc.2). Disclosure: The material characterization data and figures (e.g., UV, SEM, FTIR, XRD, TGA, Zeta Potential and particle sizer) presented here were generated from a common dataset and are being reused across multiple related studies on nanomaterials. All biological analyses and conclusions are original to each manuscript.

Conflicts of Interest: The authors declare no conflicts of interest.

REFERENCES

[1] Kunamalla R, Panagal M, Palanisamy CP. Biogenic synthesis and fabrication of starch/PVA/CuO electrospun nanoscaffolds from Sargassum ilicifolium (brown marine macroalgae) extract for anticancer activity on HT-29 and MCF-7 cancer cells. Biocatalysis and Agricultural Biotechnology. 2026; 72: 103923.

[2] Pei J, Govindaraj H, Sivaramakrishnan R, Kanniappan GV, Pandurangan V, Dhayalan VK, Mironescu M, Mironescu ID, Jayaraman S, Palanisamy PC. Sustainable fabrication of biopolymer-based (starch/PVA) nanoscaffolds loaded with green-synthesized CuO nanoparticles from Sargassum wightii (marine macroalgae): Cytocompatibility and antioxidant activity. Biomaterials Advances. 2026; 182: 214660.

[3] Pei J, Perumal NC, Meng P, Long Q, Palanisamy CP. Extracellular vesicle-based biosensors for Alzheimer's disease: A new frontier in precision diagnostics. Ageing Research Reviews. 2026; 113: 102904.

[4] Shree P, Sivaramakrishnan R, Kanniappan GV, Pandurangan V, Jayaraman S, Dhayalan VK, Mironescu M, Mironescu ID, Palanisamy CP. Antioxidant and biocompatible CuO-starch/PVA nanoscaffolds via ultrasonic green synthesis using Turbinaria conoides (brown marine macroalgae). Medicine in Drug Discovery. 2025; 28: 100238.

[5] Gong J, Lin J, Guan T, Pei J, Palanisamy CP, El-AtyFrom AMA. selenium tolerance to nanoplastic antagonism: Comprehensive characterization of L. casei SNUT1 and its extracellular vesicle–nanoselenium complex. Food Bioscience. 2025; 74: 107749.

[6] Poochi SP, Sundarraj R, Raju MV, Chandrasekaran MK, Ahalliya RM, Palanisamy CP, Kanniappan GV, Kondapavuluri BK, Thiruvengadam M. Harnessing Nature: Computational and Experimental Insights Into *Ipomoea obscura* Metabolites for Bladder Cancer Therapy. Chemistry and Biodiversity. 2025; 0: e00909.

[7] Dugganaboyana GK, Kannankumar MKG, Shivaramakrishna S, Raju MV, Chandrasekaran MK, Ahalliya RM, Panneerselvam N, Palanisamy CP, Kanniappan GV. Phytochemical insights, antioxidant activity and therapeutic potential of Cassia senna against prostate cancer in Wistar albino rats. Discover Applied Sciences. 2025; 7:1206.

[8] Natarajan SR, Krishnamoorthy R, Alshuniaber MA, Gatasheh MK, Rajagopal P, Veeraraghavan VP, Palanisamy CP, Jayaraman S. KDM1A Facilitates Oncogenic Potential in Colorectal Cancer Progression Through the Activation of AXIN/GSK3β/β-Catenin Signaling Pathways: Evidence From Integrated Transcriptomics and In Vitro Studies. The Journal of Gene Medicine. 2025; 27(11): e70053.

[9] Guan T, Gong J, Lin J, Palanisamy CP, Jinjin Pei J, El-Aty AMA. Machine learning-driven multimodal optimization of selenium biotransformation and flavor profiling in fermented apple–Yacon functional beverages. Innovative Food Science & Emerging Technologies. 2025; 105: 104198.

[10] Natarajan SR, Krishnamoorthy R, Alshuniaber MA, Alsulami TS, Gatasheh MK, Rajagopal P, Palanisamy CP, Govindan R, Veeraraghavan VP, Jayaraman S. ABCE1 facilitates tumour progression via aerobic

glycolysis and inhibits cell death in human colorectal cancer cells through the p53 signalling pathway. Scientific Reports. 2025; 15: 24674.
[11] Huang Y, Guo H, Liu Y, Jin W, Palanisamy CP, Pei J, Oz F, El-Aty AMA. Effects of Natural Polysaccharides on the Gut Microbiota Related to Human Metabolic Health. Molecular Nutrition & Food Research. 2025; 69:e202400792.
[12] Poornima K, Meenakshi K.C, Manikandan V.R, Shankari G, Prabhu D, Rathi M.A, Palanisamy CP, Balaji R, Gopalakrishnan V.K. Exploring the anticancer potential of Jerantinine A from *Tabernaemontana coronaria* against prostate, breast, and ovarian cancers: A computational approach. *Journal of Complementary and Integrative Medicine*, 2025 22(2): 363–372.
[13] Palanisamy CP, Poompradub S, Sansanaphongpricha K, Jayaraman S, Subramani K. Faridah Sonsudin gGreen synthesis of Nigella sativa-mediated silver nanoparticles for enhanced antibacterial activity and wound healing: Mechanistic insights and biomedical applications. Environmental Nanotechnology, Monitoring & Management. 2025; 24: 101085.
[14] Surendran N, Raju MV, Chandrasekaran MK, Ahalliya RM, Palanisamy CP, Chandrasekaran G, Kanniappan GV. Physicochemical characterization of starch from Maranta arundinacea L.(arrowroot) rhizomes and its inhibition of COX-2: In vivo validation. Bioactive Carbohydrates and Dietary Fibre. 2025; 33: 100465.
[15] Kannappan P, Chandrasekaran MK, Raju MV, Gopalakrishnan S, Dhamodharan P, Ahalliya RM, Palanisamy CP, Raju B, Kanniappan GV. Exploring the anticancer potential of Jerantinine A from Tabernaemontana coronaria against prostate, breast, and ovarian cancers: a computational approach. Journal of Complementary and Integrative Medicine. 2025; 22(02): 363-372.
[16] Pei J, Kumarasamy RV, Jayaraman S, Kanniappan GV, Long Q, Palanisamy CP. Quercetin-functionalized nanomaterials: Innovative therapeutic avenues for Alzheimer's disease management. Ageing Research Reviews. 2025; 104: 102665.
[17] Jayaraman S, Prasad M, Natarajan SR, Krishnamoorthy R, Alshuniaber MA, Gatasheh MK, Veeraraghavan VP, Rajagopal P, Palanisamy CP. Molecular mechanisms underlying the effects of beta-sitosterol on TGF-β1/Nrf2/SIRT1/p53-mediated signaling in the kidney of a high-fat diet and sucrose-induced type-2 diabetic rat. Chemico-Biological Interactions. 2025; 411: 111443.
[18] Huang Y, Guo H, Liu Y, Jin W, Palanisamy CP, Pei J, Oz F, El-Aty AMA. Effects of Natural Polysaccharides on the Gut Microbiota Related to Human Metabolic Health. Molecular Nutrition & Food Research. 2025; e202400792.
[19] Prabhakaran P, Palanisamy CP, Shanmugam A, Damodharan P, Swaminathan H, Devaraj D, Ahalliya RM, Kanniappan GV. Isolation, structural characterization, and molecular docking studies on the bioactive compound from n-Hexane extract of Emilia sonchifolia (L.) DC against the pancreatic cancer target Aurora 2 Kinase. Journal of Complementary and Integrative Medicine. 2024; 22(1): 0290.
[20] Jiang H, Kumarasamy RV, Pei J, Raju K, Kanniappan GV, Palanisamy CP. Integrating engineered nanomaterials with extracellular vesicles: Advancing targeted drug delivery and biomedical applications. Frontiers in Nanotechnology. 2024; 6: 1513683.
[21] Guo H, Liu Y, Wan T, Song D, Palanisamy CP, Geng J, Pei J, Özmen S, El-Aty AMA. Toward personalized cancer management: Role of precision nutrition–diet interventions. Journal of Functional Foods. 2024; 123: 106584.
[22] Natarajan SR, Krishnamoorthy R, Alshuniaber MA, Al-Anazi KM, Farah MA, Rajagopal P, Palanisamy CP, Veeraraghavan VP, Jayaraman S. Identification of FOXM1 as a novel protein biomarker and therapeutic target for colorectal cancer progression: Evidence from immune infiltration and bioinformatic analyses. International Journal of Biological Macromolecules. 282 (Part 4): 137201.
[23] Rajendran MS, Jayaraman S, Khan JM, Jasmine S, Prabhakaran RK, Raju MV, Chandrasekaran MK, Ahalliya RM, Kannappan P, Palanisamy CP, Kanniappan GV. Investigating the colon toxicity and carcinogenic role of monosodium glutamate compared with Dimethylhydrazine in male Wistar rats: Exploring the link to childhood colon cancer risk. Journal of King Saud University - Science. 2024; 36(11): 103507.
[24] Kumarasamy RV, Natarajan P, Umapathy VR, Roy JR, Rab SO, Saeed M, Panagal M, Mironescu M, Srinivasan GP, Palanisamy CP. Clinical Applications and Therapeutic Potentials of Advanced Nanoparticles: A Comprehensive Review on Completed Human Clinical Trials. Frontiers in Nanotechnology. 2024; 6:1479993.
[25] Jin W, Pei JJ, Roy JR, Jayaraman S, Ahalliya RM, Kanniappan GV, Mironescu M, Palanisamy CP. Comprehensive review on single-cell RNA sequencing: A new frontier in Alzheimer's disease research. Ageing Research Reviews. 2024; 274: 102454.
[26] Natarajan PM, Umapathy VR, Murali A, Swamikannu B. (2022). Computational Simulations of Identified marine-derived Natural Bioactive Compounds As Potential Inhibitors of Oral Cancer. Future Science OA. 2022; 8(3).
[27] Natarajan PM, Umapathy VR. Role of transcriptomics in the study of oral cancer. Frontiers in Oral Health. 2025; 6:1524364.
[28] Vidhyarekha U, Natarajan PM, Bhuminathan S, Sabarinathan J, Suba R, Vijayalakshmi P. Role of artificial intelligence in Oral Cancer. Advances in Public Health. 2024. 2024: 3664408.

[29] Ganesan A, Kumar NG, Natarajan PM, Gauthaman J. Automated classification of elongated styloid processes using deep learning models-an artificial intelligence diagnostics. Frontiers in Oral Health. 2025; 5: 1424840.
[30] Umapathy VR, Natarajan PM, Swamikannu B. Regenerative Strategies in Dentistry: Harnessing Stem Cells, Biomaterials and Bioactive Materials for Tissue Repair. Biomolecules. 2025; 15: 546.
[31] Natarajan PM. Dental Bioinformnatics-Current Scope and Future perspectives. Research Journal of Pharmacy and Technology. 2022;15(5):2351-6.
[32] Ganesan A, Kumar NG, Natarajan PM. Solanum trilobatum leaf extract-derived silver nanoparticles downregulate the PI3K/AKT/mTOR signaling pathway and attenuate oral squamous cell carcinoma cell proliferation. Journal of Herbmed Pharmacology. 2024; 13(2): 300-307.
[33] Perumal MKK, Renuka RR, Subbiah SK, Natarajan PM. Artificial intelligence-driven clinical decision support systems for early detection and precision therapy in oral cancer: a mini review. Frontiers in Oral Health. 2025; 6: 1592428.
[34] Ramesh E, Ganesan A, Lakshmi KC, Natarajan PM. Artificial intelligence-based diagnosis of oral leukoplakia using deep convolutional neural networks Xception and MobileNet-v2. Frontiers in Oral Health. 2025; 6: 1414524.
[35] Ganesan A, Kumar NG, Natarajan PM. Anticancer activity of silver nanoparticles synthesized from aqueous leaf extract of Solanum trilobatum (Purple fruit pea eggplant) on human oral cancer cells. Journal of Herbmed Pharmacololgy. 2024; 13(2): 260-268.
[36] Pei J, Palanisamy CP, Jayaraman S, Natarajan PM, Umapathy VR, Roy JR, Panagal M, Jayaraman S. Curcumin-loaded polymeric nanomaterials as a novel therapeutic strategy for Alzheimer's disease: A comprehensive review. Ageing Research Reviews. 2024; 99: 102393.
[37] Pei J, Palanisamy CP, Jayaraman S, Natarajan PM, Umapathy VR, Roy JR, Thalamati D, Ahalliya RM, Kanniappan GV, Mironescu M. A comprehensive review on starch-based Sustainable Edible Films Loaded with Bioactive Components for Food Packaging. International Journal of Biological macromolecules. 2024; 274 (Part-1): 133332.
[38] Palanisamy CP, poompradub S, Sansanaphongpricha K, Subramani K, Sonsudin F. Increased expression levels of PDGF and VEGF magnify the wound healing potential facilitated by biogenic synthesis of silver nanoparticles. Nano-Structures & Nano-Objects. 2024; 39: 101236.
[39] Pei J, Palanisamy CP, Jayaraman S, Natarajan PM, Umapathy VR, Roy JR, Thalamati D, Ahalliya RM, Kanniappan GV, Mironescu M. Proteomics Profiling of Extracellular Vesicle for Identification of Potential Biomarkers in Alzheimer's Disease: A Comprehensive Review. Ageing Research Reviews. 2024; 99: 102359.
[40] Xi J, Wang T, Xian P, Liu X, Du M, Yang H, Palanisamy CP, Lin W, Long Q. Proteomic insights uncover enhanced neurotherapeutic potential in conditioned mesenchymal stem cell-derived extracellular vesicles. Extracellular Vesicle. 2024; 3: 100037.
[41] Pei J, Natarajan PM, Umapathy VR, Swamikannu B, Sivaraman NM, Krishnasamy L, Palanisamy CP. Advancements in the synthesis and functionalization of zinc oxide-based nanomaterials for enhanced oral cancer therapy. Molecules. 2024; 29(11): 2706.
[42] Gatasheh MK, Natarajan SR, Krishnamoorthy R, Alsulami TS, Rajagopal P, Palanisamy CP, Veeraraghavan VP, Jayaraman S. Molecular analysis to identify novel potential biomarkers as drug targets in colorectal cancer therapy: an integrated bioinformatics analysis. Molecular and Cellular Oncology. 2024; 11(1): 2326699.
[43] Pei J, Yan Y, Jayaraman S, Rajagopal P, Natarajan PM, Umapathy VR, Gopathy S, Roy JR, Sadagopan CS, Thalamati D, Palanisamy CP, Mironescu M. A review on advancements in the application of starch-based nanomaterials in biomedicine: Precision drug delivery and cancer therapy. International Journal of Biological Macromolecules. 2024; 130746.
[44] Pei JJ, Yan Y, Palanisamy CP, Jayaraman S, Natarajan PM, Umapathy VR, Gopathy S, Roy JR, Sadagopan JC, Thalamati D, Mironescu M. Materials-based drug delivery approaches: Recent advances and future perspectives. Green Processing and Synthesis. 2024; 13: 20230094.
[45] Pei JJ, Deng W, Liu Y, Guo Y, Chen J, Abdu H, Khan MR, Palanisamy CP, El-Aty AM. A Comprehensive Review of Cornus officinalis: Health Benefits, Phytochemistry, and Pharmacological Effects for Functional Drug and Food Development. Frontiers in Nutrition. 2023; 10: 1309963.
[46] Alugoju P, Palanisamy CP, Anthikapalli NVA, Jayaraman S, Prasanskulab A, Chuchawankul S, Dyavaiah M, Tencomnao T. Exploring the anti-aging potential of natural products and plant extracts in budding yeast Saccharomyces cerevisiae: A review. F1000Research. 2023; 12: 1265.
[47] Lavanya M, Krishnamoorthy R, Alshuniaber MA, Manoharadas S, Palanisamy CP, Veeraraghavan VP, Jayaraman S, Rajagopal P, Padmini R. Formulation, characterization and evaluation of gelatin-syringic acid/zinc oxide nanocomposite for its effective anticancer, antioxidant and anti-inflammatory activities. Journal of King Saud University-Science. 2023; 35: 102909.
[48] Palanisamy CP, Poompradub S, Sansanaphongpricha K, Jayaraman S, Subramani K, Sonsudin F. Biosynthesis of silver nanoparticles (AgNPs) using ethanolic extract of Nigella sativa (L.) seeds promotes wound healing via PDGF and VEGF signalling pathways activation. Biocatalysis and Agricultural Biotechnology. 2023; 54: 102970.

[49] Prasad M, Jayaraman S, Natarajan SR, Veeraraghavan VP, Krishnamoorthy R, Gatasheh MK, Palanisamy CP, Elrobh M. Piperine modulates IR/Akt/GLUT4 pathways to mitigate insulin resistance: Evidence from animal and computational studies. International Journal of Biological Macromolecules. 2023; 253: 127242.
[50] Palanisamy CP, Pei JJ, Phaniendra A, Venkata AAN, Jayaraman S, Veeraragahavan VP, Sridevi G, Roy JR, Janaki CS, Thalamati D, Mironescu M, Luo Q, Chai Y, Long Q. New Strategy of Neurodegenerative Disease Treatment with Extracellular Vesicles (EVs) Derived from Mesenchymal Stem Cells (MSCs). *Theranostics*. 2023; 13(12):4138-4165. doi:10.7150/thno.83066.
[51] Palanisamy CP, Phaniendra A, Jayaraman S, Poompradub S. *Nigella sativa* L. seed extracts promotes wound healing progress by activating VEGF and PDGF signalling pathways: *An in vitro* and *in silico* study. *F1000 Research*. 2023; 12: 436.
[52] Pei JJ, Palanisamy CP, Phaniendra A, Venkata AAN, Natarajan PM, Umapathy VR, Swamikannu B, Jayaraman S, Rajagopal P, Poompradub S. A comprehensive review on bio-based materials for chronic diabetic wounds. *Molecules*. 2022; 28(2), 604.
[53] Palanisamy CP, Cui B, Zhang H, Gunasekaran VP, Ariyo A, Jayaraman S, Veeraraghavan V, Rajagopal P. A critical review on starch-based electrospun nanofibrous scaffolds for wound healing application. International Journal of Biological Macromolecules. 2022; 222 (Part: B): 1852-1860.
[54] Monisha P, Ponnulakshmi R, Nalini D, Vishnu P V, Palanisamy CP, Cui B, Shankargouda P, Selvaraj J. A comprehensive review on high fat diet-induced diabetes mellitus: An epigenetic view. The Journal of Nutritional Biochemistry. 2022; 2022: 109037.
[55] Monisha P, Selvaraj J, Mohamed AE, Mohamed E, Mosaab AEA, Vishnu PV, Srinivasan V, Vidhya RU, Shazia FJH, Kalaiselvi K, Durairaj S, Palanisamy CP, Surapaneni K M, Ponnulakshmi R. A Comprehensive review on therapeutic perspectives of phytosterols in insulin resistance: A mechanistic approach. Molecules. 2022; 27(5): 1595.
[56] Natarajan PM, Swamikannu B, Sivaraman NM, Stylin AGSQ. Prevention of Oral Cancer: A Comprehensive Guide. Journal of Pharmacy and Bioallied Sciences. 2024; 16(5): S4239-S4241.
[57] Umapathy V, Dhanavel A, Kesavan R, Natarajan PM, Bhuminathan S, Vijayalakshmi P. Anticancer Potential of the Principal Constituent of Piper nigrum, Piperine: A Comprehensive Review. Cureus. 2024; 16(2): e54425.
[58] Umapathy VR, Swamikannu B, Natarajan PM, Devi R, Nandini MS, Vimalarani, Vijayalakshmi P. In Silico Molecular Docking of Ocimum sanctum Phytochemicals: Targeting Key Biomarkers in Oral Cancer. Journal of Pharmacy and Bioallied Sciences. 2024; 16(5): S4792-S4799.
[59] Natarajan PM, Bhuminathan S, Rajan R, Bindu K, Loganathan K, Veerakumar R. The Crucial Role of Smoking Cessation in Preventing Oral Cancer. Journal of Pharmacy and Bioallied Sciences. 2024; 16(5): S4245-S4247.
[60] Swamikannu B, Umapathy VR, Natarajan PM, Nandini MS, Stylin AGSQ, Vimalarani V, Rajinikanth S. Unlocking the Therapeutic Benefits of Artemisia Annua: A Comprehensive Overview of its Medicinal Properties. Journal of Pharmacy and Bioallied Sciences. 2024; 16(5): S4248-S4253.
[61] Natarajan PM. Computational Studies on Recent Congeners of Fluoroquinolones and Nitroimidazoles for Their Use in Periodontal Therapy. Journal of Pharmacy and Bioallied Sciences. 2024; 16(5): S4731-S4740.
[62] Yadalam PK, Arumuganainar D, Natarajan PM, Ardila CM. Artificial intelligence-powered prediction of AIM-2 inflammasome sequences using transformers and graph attention networks in periodontal inflammation. Scientific Reports. 2025; 15: 8733.
[63] Yadalam PK, Chatterjee S, Natarajan PM, Ardila CM. Comparison of light gradient boosting and logisti c regression for interactomic hub genes in Porphyromonas gingivalis and Fusobacterium nucleatum-induced peri odontitis with Alzheimer's disease. Frontiers in Oral Health. 2025; 6:1463458.
[64] Natarajan PM, Bhuminathan S, Leela B, Bindu K, Loganathan K, Ramachandran V. Smoking and its Role in Oral Cancer. Journal of Pharmacy and Bioallied Sciences 16(5): S4242-S4244.
[65] Yadalam PK, Natarajan PM, Ardila CM. Variational graph autoencoder for reconstructed transcriptomic data associated with NLRP3 mediated pyroptosis in periodontitis. Scientific Reports. 2025; 15: 1962.
[66] Pei JJ, Perumal NC, Meng P, Long Q, Palanisamy CP. AI-assisted FTIR spectroscopic profiling of exosomes: Emerging frontiers in early detection of Alzheimer's disease. Ageing Research Reviews. 2026; 103311.
[67] Raja FSD, Abraham L, Rangasamy K, Saikia K, Rathankumar AK, Mironescu M, Mironescu I, Palanisamy CP, Kanniappan GV. Next-Generation Microbiome Therapeutics: Psychobiotics and Fecal Microbiota Transplants (FMT) for Mental Health Treatment. Frontiers in Cellular and Infection Microbiology. 2026; 16: 1719357.
[68] Subramani K, Srinivasan S, Shanmugam P, Palanisamy CP, Sonsudin F, Poompradub S. Sustainable phytochemical mediated-ZnO nanoparticles derived from Crescentia cujete for toxicological evaluation and multifunctional environmental applications. Environmental Nanotechnology, Monitoring & Management. 2026; 26: 101180.
[69] Kunamalla RP, Panagal M, Palanisamy CP. Green-engineered multiscale starch/PVA nanofibrous scaffolds embedded with CuO nanoparticles from Sargassum ilicifolium for potent antimicrobial performance. Genetics and Molecular Research. 2026; 25(13s): 1-9.

[70] Dharmaprakash S, Gunasekaran VP, Sivaramakrishnan R, Kanniappan GV, Jayaraman S, Mironescu M, Rajabathar JR, Mironescu ID, Palanisamy CP. Marine macroalgae-mediated ultrasonic-assisted green synthesis of CuO nanoparticles embedded in starch/PVA electrospun nanoscaffolds for in vitro α-amylase and α-glucosidase inhibitory activity. Scientific Reports. 2026; 16: 26243.
[71] Surendran N, Chandrasekaran G, Raju MV, Chandrasekaran MK, Ahalliya RM, Palanisamy CP, Kanniappan GV, Arcot R, Alharbi NS, Thiruvengadam M. Anti-inflammatory potential of ethanolic extract of Maranta arundinacea L.: Insights from COX-2 modulation and oxidative stress analysis. South African Journal of Botany. 2026; 195: 142-151.
[72] Pei J, Senthilkumar MV, Hessini K, Subramaniyam S, Sivaramakrishnan R, Kanniappan GV, Jayaraman S, Palanisamy CP. Green fabrication of starch/PVA/CuO nanoscaffolds using marine macroalgae extract for enhanced anti-inflammatory activity. Sustainable Chemistry and Pharmacy. 2026; 51: 102397.
[73] Balasubramanian V, Loganathan L, Muthuswamy K, Viswanathan TM, Raju MV, Chandrasekaran MK, Ahalliya RM, Poorasamy J, Palanisamy CP, Dominic S, Kanniappan GV. Anticancer therapeutic efficacy of PEGylated β-galactosidase from Aspergillus terreus in DMBA-induced breast cancer: Toxicological, molecular and histopathological evaluation in Wistar rats. International Journal of Biological Macromolecules. 2026; 360: 151856.
[74] Jayaraman S, Eswaran A, Rajagopal P, Palanisamy CP, Veerakumar P, Veeraraghavan VP, Sirasanagandla SR. Neuroendocrine-associated epigenetic factors in cellular senescence: mechanisms and therapeutic implications. Biogerontology. 2026; 27(2): 64.
[75] Jayakumar M, Senthil P, Suganthirababu P, Ramalingam V, Palanisamy CP. Longitudinal effects of body weight supported gait training on functional gait recovery after stroke: A pilot randomized controlled trial. Genetics and Molecular Research. 2026; 25(12s): 2026.
[76] Ponnusamy B, Rajagopal P, Palanisamy CP, Veeraraghavan VP, Jayaraman S. Mechanistic Exploration of the anticancer activity of Justicia adhatoda Plant Leaf Ethanolic Extract against Colon Cancer Cells: An in silico and in vitro Approach. Asian Pacific Journal of Cancer Prevention. 2026; 27(3): 1069-1080.
[77] Pei J, Saran VS, Sivaramakrishnan R, Kanniappan GV, Pandurangan V, Jayaraman S, Dhayalan VK, Mironescu M, Mironescu ID, Palanisamy CP. Ultrasonic-assisted, Sargassum ilicifolium (brown marine macroalgae)-mediated biogenic synthesis of CuO nanoparticles incorporated in starch/PVA electrospun nanoscaffolds: In vitro safety and antioxidant efficacy assessment. Bioorganic Chemistry. 2026; 173: 109679.
[78] Raj MAPA, Subramaniyam S, Kanniappan GV, Jayaraman S, Palanisamy CP. Sustainable fabrication of starch/PVA/CuO electrospun nanoscaffolds from Turbinaria ornata (marine macroalgae) extract: Physicochemical characterization and antidiabetic evaluation. Kuwait Journal of Science. 2026; 53(2): 100545.
[79] Pei J, Ganesh NS, Subramaniyam S, Sivaramakrishnan R, Kanniappan GV, Jayaraman S, Palanisamy CP. Sustainable fabrication of starch/PVA/CuO electrospun nanoscaffolds from Padina tetrastromatica (Brown macroalgae) extract: Physicochemical characterization and antidiabetic assessment. Sustainable Chemistry One World. 2026; 9: 100195.
[80] Sakthiraj A, Sivaramakrishnan R, Subramaniyam S, Kanniappan GV, Pandurangan V, Jayaraman S, Dhayalan VK, Mironescu M, Mironescu ID, Palanisamy CP. Starch/PVA electrospun nanoscaffolds loaded with ultrasonic-assisted green-synthesis of CuO nanoparticles from marine macroalgae (Gracilaria corticata) extract: Cytotoxicity and antioxidant analysis. Chemical Physics Impact. 2026; 12: 101018.
[81] Raju M, Chandrasekaran MK, Loganathan L, Ahalliya RM, Mironescu M, Mironescu ID, Palanisamy CP, Kanniappan GV. Lipid remodeling and ferroptosis in phosphatidylcholine-mediated tumor–stroma crosstalk. Frontiers in Molecular Biosciences. 2026; 13: 1742305.